$d \quad = k_4 \cos\phi$

$$c'' = \frac{\omega^2 k_{6d}/\omega_r^2}{1 - \omega^2/\omega_r^2(1 + ig_6)}$$

l_0 and ϕ are defined by Fig. 1. Any particular element can be removed from the point transfer matrix by setting the appropriate stiffness to zero.

References

[1] Miles, J. W., "Vibrations of Beams on Many Supports," *Journal of the Engineering Mechanics Division, American Society of Civil Engineers*, Vol. 82, No. EM1, Jan. 1956, pp. 1–9.

[2] Lin, Y. K., "Free Vibrations of a Continuous Beam of Elastic Supports," *International Journal of Mechanical Sciences*, Vol. 4, No. 5, Sept.–Oct. 1962, pp. 409–423.

[3] Wah, T., "Natural Frequencies of Uniform Grillages," *Journal of Applied Mechanics*, Vol. 30, No. 4, Dec. 1963, pp. 571–578.

[4] Lin, Y. K., Brown, I. D., and Deutschle, P. C., "Free Vibrations of a Finite Row of Continuous Skin-Stringer Panels," *Journal of Sound and Vibration*, Vol. 1, No. 1, Jan. 1964, pp. 14–27.

[5] Wah, T., "Flexural Vibrations of Ring-Stiffened Cylindrical Shells," *Journal of Sound and Vibration*, Vol. 3, May 1966, pp. 242–251.

[6] Lin, Y. K., "Free Vibration of Continuous Skin-Stringer Panels," *Journal of Applied Mechanics*, Vol. 27, No. 4, Dec. 1960, pp. 669–676.

[7] Schnell, W. and Heinrichsbauer, F., "Zur Bestimmung Der Eigenschwingungen Langsversteifter, Dunnwandiger Kreiszylinderschalen," *Jahrbuch der Wissenschaftliche Gesellschaft für Luft und Raumfahrt*, 1963, pp. 278–286.

[8] Lin, Y. K. and McDaniel, T. J., "Dynamics of Beam-Type Periodic Structures," *Journal of Engineering for Industry*, Vol. 91, No. 4, Nov. 1969, pp. 1133–1141.

[9] Pestel, E. C. and Leckie, F. A., *Matrix Methods in Elastomechanics*, McGraw-Hill, New York, 1963.

[10] Lin, Y. K. and McDaniel, T. J., "Response of Multi-Spanned Beam and Panel Systems under Noise Excitation," AFML-TR-64-348, Part II, Sept. 1967, Air Force Materials Lab., Wright-Patterson Air Force Base, Ohio.

[11] Clarkson, B. L. and Cicci, F., "Methods of Reducing the Response of Integrally Stiffened Structures to Random Pressures," *Journal of Engineering for Industry*, Vol. 91, No. 4, Nov. 1969, pp. 1203–1209.

[12] Jones, D. I. G., Henderson, J. P., and Bruns, G. H., "Use of Tuned Viscoelastic Dampers for Reduction of Vibrations in Aerospace Structures," *Proceedings of the 13th Annual Air Force Symposium*, Air Force Systems Command, Arnold Air Force Station, Tenn., Vol. 1, Paper 18, 1966.

[13] Schrumpich, G., "Beitrag zur Kinetik and Statik ebener Stabwerke mit gekrummten Staben," *Osterreichisches Ingenier-Archiv*, Vol. 11, 1957, pp. 194–225.

[14] Lin, Y. K. et al., "Free Vibration of Continuous Skin-Stringer Panels with Non-uniform Stringer Spacing and Panel Thickness," AFML-TR-64-348, Part I, Feb. 1965, Air Force Materials Lab., Wright-Patterson Air Force Base, Ohio.

[15] Doi, K. and Lin, Y. K., "Spatial Decay in the Response of Damped Periodic Structures," AFML-TR-69-308, Nov. 1969, Air Force Materials Lab., Wright-Patterson Air Force Base, Ohio.

MARCH 1971 J. AIRCRAFT VOL. 8, NO. 3

Dynamic Analysis of Stiffened Panel Structures

R. N. Yurkovich*
McDonnell Douglas Corporation, St. Louis, Mo.

AND

J. H. Schmidt† and A. R. Zak‡
University of Illinois, Urbana, Ill.

The dynamic behavior of stiffened flat panels is analyzed using the method of finite-elements. The panels are stiffened by one or two sets of stiffeners which divide the panel into rectangular bays simulating a typical aircraft skin-frame-stringer configuration. The analysis is designed to investigate the free and the forced vibration behavior. In the case of the forced vibration, both undamped and damped response is examined where the damping is provided by viscoelastic dampers attached to the surface of the panel. The finite-element method consists of representing the panel by triangular plate elements, and the stiffeners are represented by beam elements which allow for bending, torsional, and warping effects. The latter effect is found to be very important. Examples are given, illustrating the application of the analysis to free and forced vibration problems. In the case of the latter, the effect of viscoelastic damping is examined and compared with experimental data. This data were obtained from an experimental investigation that was carried out in support of the theoretical analysis.

Nomenclature

A = matrix defined in Eq. (2)
A_1–A_9 = nine unknown coefficients in Eq. (1)
B = matrix defined in Eq. (8)
B_1–B_8 = eight coefficients in Eqs. (15) and (16)
C = matrix defined in Eq. (21)
C_{ws} = warping constant
D',D'' = real and imaginary parts of matrix defined in Eq. (32)
E = Young's modulus

Received February 24, 1970; revision received August 14, 1970. This work was sponsored by the Air Force Materials Laboratory, Air Force Systems Command under contract Number F33615-67-C-1190 at the University of Illinois.

* Structural Engineer. Associate Member AIAA.

† Graduate Student, Aeronautical and Astronautical Engineering Department. Member AIAA.

‡ Professor, Aeronautical and Astronautical Engineering Department. Member AIAA.

$[E]$ = matrix defined in Eq. (10)
E^* = complex modulus of viscoelastic damper
E', E'' = real and imaginary parts of E^*
F = force matrix
F_e = external force matrix
F_{1e}, F_{2e} = parts of matrix F_e defined in Eq. (34)
F_d = damping force matrix
F_z = force in z direction at ends of finite elements
G = shear modulus
$[G]$ = matrix defined in Eq. (5)
H = matrix defined in Eq. (21)
h = panel thickness
I = effective moment of inertia of stiffeners
J = St. Venant torsional constant
$[J]$ = matrix defined in Eq. (2)
K = stiffness matrix
K_1–K_4 = parts of K
L = length of finite elements for stiffeners
M = mass matrix
M_1–M_4 = parts of M
M_d = damper mass
M_x, M_y = moments acting on finite elements
m = mass of stiffeners per unit length
q = displacement matrix
$\bar{q}$ = amplitude of q
q_1, q_2 = parts of $\bar{q}$
q_{1R}, q_{1I} = real and imaginary parts of q_1
R = matrix defined in Eq. (37)
S = area of triangular panel element
t = time
U_s = strain energy
V = volume
v = displacement of the mass in the damper
w = transverse displacement of panel
X, Y = number of nodes in x and y directions
x, y, z = Cartesian coordinates
α = warping displacement
$\epsilon_x, \epsilon_y, \gamma_{xy}$ = strains
ϵ = matrix defined in Eq. (8)
θ_x, θ_y = rotations of finite element corners
ν = Poisson's ratio
ρ = density of panel per unit area
σ = matrix defined in Eq. (9)
$\sigma_x, \sigma_y, \tau_{xy}$ = stresses
ω = frequency

Subscripts

i, j, k = indicate corners in a triangular finite element
i, j = indicate ends of stiffener finite elements

Introduction

THE present analysis will be concerned with the dynamic behavior of stiffened flat panel structural models. Such models are of practical interest because they represent actual aircraft structures. In the present analysis we shall consider both the free and forced vibration behavior. In the case of the forced vibration problem, we shall consider both the undamped and damped configurations where the damping will be provided by tuned viscoelastic, discrete dampers attached to the panel surface. The model to be considered consists of a flat panel stiffened by two sets of mutually perpendicular, parallel stiffeners which divide the panel into a set of rectangular panels.

A number of previous investigations have been concerned with the dynamic analysis of stiffened panel structures.[1–7] One of the more extensively investigated problems in this area has been the behavior of a simplified model consisting of a rectangular panel stiffened by one set of parallel stiffeners. If the boundaries of the panel perpendicular to the direction of the stiffeners are assumed to be simply supported, then the analysis can be reduced to a one-dimensional problem for which an exact analytical solution is possible. This approach has been successfully applied in conjugation with the transfer matrix techniques to analyze a number of different problems in this area.[2–4,8,9] In contrast, the more general problem consisting of a panel stiffened by orthogonal stiffeners is a much more difficult mathematical problem for which exact solutions are not possible. The solution for such a problem, therefore, has to be obtained by approximate or numerical techniques, and a number of such methods have been used. These methods include infinite series solution of equilibrium equations, assumed mode methods, and numerical techniques based on finite-element analysis. Perhaps the most versatile of these methods, and the one which has been used most extensively, is the finite-element approach.[6,7,10,11] We shall, therefore, make use of this method in the present analysis.

Previous investigations in this area have made certain simplifying assumptions as to the behavior of the stiffeners, mainly that the stiffeners are infinitely rigid in bending,[7] or that torsional effects can be neglected,[6] or that warping effects are negligible.[6] For certain geometrical configurations, various of these assumptions are valid; however, this is not always true. One of the most common assumptions has been in regard to the warping effects which have either been neglected completely[6] or included empirically by defining effective torsional stiffeners.[7] It can easily be illustrated, however, that for stiffeners with open sections, such as are often used in aircraft construction, the warping is a very important factor in the dynamic response. Consequently, in the present analysis, we shall avoid making any limiting assumptions and will explicitly include the bending, torsional, and warping effects in the treatment of the stiffeners.

The aim of the present analysis will be to examine the natural frequency and the corresponding mode shapes of free vibration, and the frequency response. In the case of the forced vibration analysis we shall consider both undamped and damped structural models. The damping will be provided by viscoelastic tuned dampers attached to the surface of the panel.

In addition to the theoretical investigation of this problem, an experimental program was undertaken to provide a check for some of the theoretical results. In this investigation a stiffened panel model is subject to a sinusoidal forcing function and the frequency response is measured for undamped and damped conditions.

Analysis

Finite-Element Analysis of the Panel

The rectangular panel is divided into a set of triangular elements joined at the nodal points as shown in Fig. 1. The stiffeners are also shown in this figure; they are divided into a set of finite beam elements. The triangular grid of panel elements is chosen in size so as to start and end at the stiffeners, and both the panel and the beam elements have common end points which are called the nodes. In this arrangement the nodal points form a rectangular grid X, Y in size where X and Y are the number of nodes in the x and y directions, respectively. In this section we will consider the analysis of the panel elements.

The stiffness and the mass matrix for each individual triangular element are obtained by using the principle of virtual work. Consider a typical triangular element with nodal coordinates, nodal displacements (meaning both linear and rotational quantities), and forces as defined in Fig. 2. The transverse displacement of the panel is assumed in a polynomial form as follows[11]:

$$w = A_1 + A_2x + A_3y + A_4x^2 + A_5y^2 + A_6x^2y + A_7xy^2 + A_8x^3 + A_9y^3 \quad (1)$$

where A_1–A_9 are unknown coefficients.

Equation (1) can be written in a matrix form:

$$w = [J]\{A\} \quad (2)$$

where the matrix A contains the unknown coefficients in Eq.

(1) and J is a row matrix whose elements are functions of x and y.

Assuming plate theory, the nodal rotations can be related to the displacement w by the following equations:

$$\begin{aligned} \theta_y &= -\,\partial w/\partial x \\ \theta_x &= \partial w/\partial y \end{aligned} \tag{3}$$

Using Eqs. (1) and (3) it follows that

$$\begin{aligned} \theta_y &= -\,(A_2 + 2A_4 + 2A_6xy + A_7y^2 + 3A_8x^2) \\ \theta_x &= A_3 + 2A_5y + A_6x^2 + 2A_7xy + 3A_9y^2 \end{aligned} \tag{4}$$

Equations (1) and (4) are now used to relate the corner displacements of the triangular element in Fig. 2 to the nine unknown coefficients A_1–A_9. This relation is written in a matrix form:

$$\{q\} = [G]\{A\} \tag{5}$$

where the column matrix is defined as follows:

$$\{q\} = \{w_i,\theta_{yi},\theta_{xi},w_j,\theta_{yj},\theta_{xj},w_k,\theta_{yk},\theta_{xk}\} \tag{6}$$

In Eq. (6) the subscripts i, j, and k are used to indicate the displacements of the three different corners of the triangular element in Fig. 2.

In the analysis the panel will be treated on the basis of thin plate theory and therefore the strain-displacement relations are

$$\epsilon_x = -\,z\partial^2w/\partial x^2 \tag{7a}$$

$$\epsilon_y = -\,z\partial^2w/\partial y^2 \tag{7b}$$

$$\gamma_{xy} = -\,2z\partial^2w/\partial x\partial y \tag{7c}$$

Using Eqs. (1), (5), and (7), we can express the strains in a matrix form:

$$\{\epsilon\} = \begin{Bmatrix} \epsilon_x \\ \epsilon_y \\ \gamma_{xy} \end{Bmatrix} = [B][G]^{-1}\{q\} \tag{8}$$

where minus one superscript indicates a matrix inverse.

Introducing the elastic stress-strain relations, we can write them,

$$\{\sigma\} = \begin{Bmatrix} \sigma_x \\ \sigma_y \\ \tau_{xy} \end{Bmatrix} = E\begin{bmatrix} \dfrac{1}{1-\nu^2} & \dfrac{\nu}{1-\nu^2} & 0 \\ \dfrac{\nu}{1-\nu^2} & \dfrac{1}{1-\nu^2} & 0 \\ 0 & 0 & \dfrac{1}{2(1+\nu)} \end{bmatrix} \begin{Bmatrix} \epsilon_x \\ \epsilon_y \\ \gamma_{xy} \end{Bmatrix} \tag{9}$$

Using Eqs. (8) and (9), we can write the relation between the corner displacements and the stress in the panel element as follows:

$$\{\sigma\} = [E][B][G]^{-1}\{q\} \tag{10}$$

where $[E]$ now denotes the product of the Young's modulus and the square matrix in Eq. (9).

The equilibrium equations for the triangular element are developed by using the principle of virtual work. The details of this method will be omitted since they are well known and can be found in previous literature.[10] This procedure leads to the following nine equations of motion:

$$[M]\{\ddot{q}\} + [K]\{q\} = \{F\} \tag{11}$$

The mass and the stiffness matrices in Eq. (11) are

$$[M] = \rho\int_s [G]^{-1T}\{J\}[J][G]^{-1}dS \tag{12}$$

and

$$[K] = \int_V [g]^{-1T}[B]^T[E][B][G]^{-1}dV \tag{13}$$

The superscript T in Eqs. (12) and (13) indicates a matrix transform. The force matrix in Eq. (11) is defined as

$$\{F\} = \{F_{zi},M_{yi},M_{xi},F_{zj},M_{yj},M_{xj},F_{zk},M_{yk},M_{xk}\} \tag{14}$$

The forces in Eq. (14) are defined in Fig. 2.

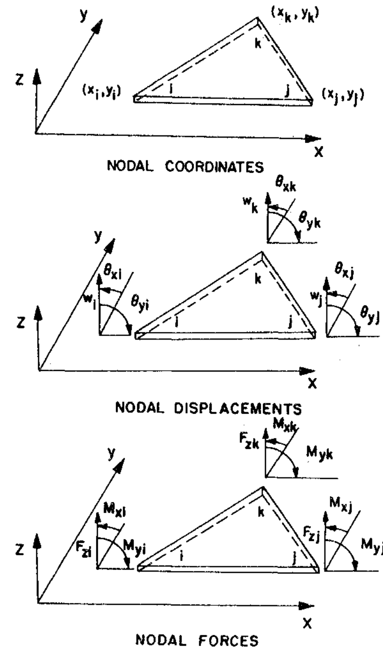

Fig. 2 Nodal coordinates, displacements and forces acting on a triangular panel element.

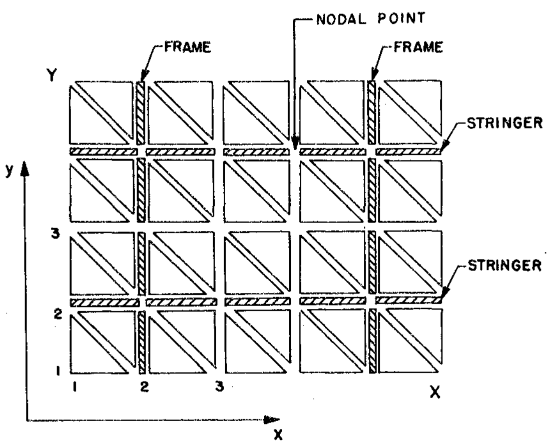

Fig. 1 Finite-element representation of a panel-stringer-frame structural model.

Finite-Element Analysis of the Stiffeners

In this section the equilibrium equations for the stiffener beam elements, shown in Fig. 1, will be developed. This analysis will be analogous to the one in the last section for the panel elements. Figure 3 shows the end displacement and forces on a representative beam element. The displacements are composed of one linear displacement in the z direction, two rotations, and a warping displacement. Corresponding to these displacements, there are four forces. The beam can undergo bending and rotational displacements, and the first step of the analysis is to assume polynomial expressions for these two displacements. The bending displacement is assumed in the following form:

$$w = B_1 + B_2x + B_3x^2 + B_4x^3 \tag{15}$$

and the rotational displacement is represented by

$$\theta_x = B_5 + B_6x + B_7x^2 + B_8x^3 \tag{16}$$

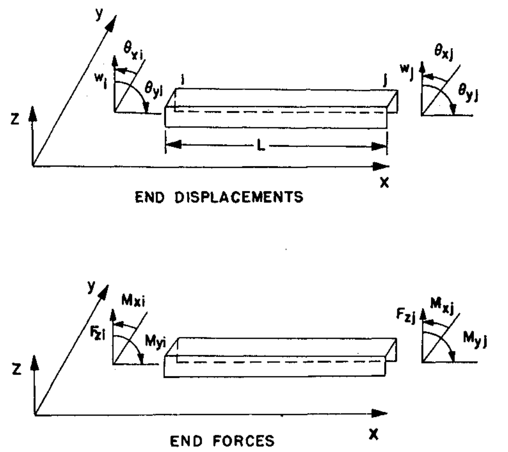

Fig. 3 End displacements and forces acting on a beam element.

The eight quantities B_1–B_8 defined in Eqs. (15) and (16) are unknown coefficients. The rotation θ_x is used here to denote the rotation of the stiffener along the line at which the stiffener is attached to the panel.

The rotation θ_y, shown in Fig. 3, is related to the displacement w by the relation

$$\theta_y = -\partial w/\partial x \tag{17}$$

Using Eqs. (15) and (17), we obtain

$$\theta_y = -(B_2 + 2B_3x + 3B_4x^2) \tag{18}$$

The warping displacement is denoted by α, and it represents the magnitude of a warping strain which is a normal strain varying over the cross section of the stiffener. The magnitude of the strain is proportional to the second derivative of the rotation along the length of the beam, and therefore it is convenient to use this derivative as the definition of α:

$$\alpha = \partial^2\theta_x/\partial x^2 \tag{19}$$

Using Eqs. (16) and (19) it follows that

$$\alpha = 2B_7 + 6B_8x \tag{20}$$

It is convenient at this point to consider the physical meaning of the warping force N in the beam element. The warping strain produces a normal stress over the cross section of the beam whose magnitude is proportional to the magnitude of the warping strain. This warping stress varies over the beam cross section and is self-equilibrating, since it produces zero axial load and zero bending. The warping force N is used here as quantity proportional to magnitude of this warping stress.

Using Eqs. (15), (16), (18), and (20), all the displacements at both ends of the beam element can be related to the eight unknown coefficients B_1–B_8 by the following matrix equation:

$$\{q\} = [C]\{H\} \tag{21}$$

where the matrix H is a column matrix of the unknown coefficients and matrix q is defined as follows:

$$\{q\} = \{w_i,\theta_{yi},\theta_{xi},w_j,\theta_{yj},\theta_{xj},\alpha_i,\alpha_j\} \tag{22}$$

The subscripts i and j in Eq. (22) indicate the quantities belonging to i and j ends of the beam shown in Fig. 3. Equation (21) is inverted to give the coefficients in terms of the end displacements:

$$\{H\} = [C]^{-1}\{q\} \tag{23}$$

The total strain energy of the beam element is composed of bending, torsional, and warping components, and is given by the following equation:

$$U_s = \frac{1}{2}\int_0^L EI\left(\frac{\partial^2 w}{\partial x^2}\right)^2 dx + \frac{1}{2}\int_0^L GJ\left(\frac{\partial\theta_x}{\partial x}\right)^2 dx + \frac{1}{2}\int_0^L EC_{ws}\left(\frac{\partial^2\theta_x}{\partial x^2}\right)^2 dx \tag{24}$$

The strain energy given by Eq. (24) can be expressed by a quadratic function of the eight coefficients B_i–B_8, which in turn can be converted by using Eq. (23) to a quadratic in the end displacements given by the matrix q. Again applying the principle of virtual work and equating virtual work to virtual change in strain energy, we obtain eight equations of equilibrium for each stiffener element. These equations have the same general form as Eq. (11).

Equations of Motion for the Total Structure

From the matrix equations of motion for the individual panel and beam elements, the corresponding equations for the total stiffened structure are obtained by satisfying force equilibrium and displacement compatibility at each nodal point. The resulting equation has the form

$$[M]\{\ddot{q}\} + [K]\{q\} = \{F_e\} \tag{25}$$

In the Eq. 25 F_e matrix represents external forces applied at the nodes. It may be noted that Eq. (25) has the same general form as Eq. (11), except the matrices M, K, and q refer now to the total structure.

Equation (25) will be used in the following sections to investigate the free and the forced vibration problems.

Application to Free Vibration Analysis

In this section we shall consider the free vibration case and use the present analysis to determine the natural frequencies and modes for a stiffened structure. In case of free vibration the external force matrix in Eq. (25) is zero and the motion can be represented by an exponential form:

$$\{q\} = \{\bar{q}\}e^{i\omega t} \tag{26}$$

where ω is the natural frequency and $\bar{q}$ is the corresponding natural mode. Since q will not appear further in the analysis, we shall use this symbol in place of $\bar{q}$ for simplicity. Not all of the displacements in q have to be unknown and some of these can be specified as zero by the boundary conditions. It is convenient to denote the unknown displacements by q_1 and the known by q_2, and rearrange the order of q in Eq. (26) to put the specified displacements at the end of the matrix. Using Eq. (26) in Eq. (25) and partitioning the mass and the stiffness matrices, we obtain a set of algebraic equations:

$$-\omega^2\left[\begin{array}{c|c} M_1 & M_2 \\ \hline M_3 & M_4 \end{array}\right]\begin{Bmatrix} q_1 \\ q_2 \end{Bmatrix} + \left[\begin{array}{c|c} K_1 & K_2 \\ \hline K_3 & K_4 \end{array}\right]\begin{Bmatrix} q_1 \\ q_2 \end{Bmatrix} = 0 \tag{27}$$

Since the displacements q_2 are zero, Eq. (27) reduces to the following form after inverting K_1 matrix:

$$\{q_1\} = \omega^2[K_1]^{-1}[M_1]\{q_1\} \tag{28}$$

The solution of Eq. (28) is obtained on a digital computer by using the matrix iteration method. The computational procedure is designed to calculate the three lowest natural frequencies and the corresponding mode shapes. Examples of the application of this analysis will be given later.

Application to Undamped and Damped Forced Vibration Analysis

The forced vibration analysis is designed to obtain the frequency response of undamped and damped structures. The damping is assumed to be provided by a damper attached to the panel surface and which generates damping force in the z direction. The damper is composed of a viscoelastic element one end of which is attached to the panel and the other end to a mass M_d as shown in Fig. 4. Under harmonic load, the viscoelastic properties of the damper are represented by a dynamic modulus E^* which is a complex function whose real part is usually called the storage and the imaginary part the loss modulus. We define these quantities by the relation

$$E^* = E' + iE'' \tag{29}$$

Under sinusoidal conditions, the equation of motion for the viscoelastic damper is given by the relation

$$-\omega^2 M_d v = E^*(v - w) \tag{30}$$

where v is the deflection of the damper mass. Using Eq. (32), the damping force between the damper and the panel can be written as

$$F_d = E^*\omega^2 M_d/(E^* - \omega^2 M_d)w \tag{31}$$

Considering the dampers to be present at an arbitrary number of nodes, Eq. (31) can be written in a matrix form:

$$\{F_d\} = [D' + iD'']\{q\} \tag{32}$$

where D' and D'' are real and the imaginary parts of elements of a diagonal matrix.

In the present analysis the dampers are assumed to be located at the nodal points on the structure. This is not a severe restriction since the nodal pattern is quite flexible. The damping force given by Eq. (32) can be included on the right-hand side of Eq. (25) as a part of the external force, and the force F_e will now be used to denote any additional loads on the structure not including damping forces. Assuming harmonic excitation, Eq. (25) can be written as

$$-\omega^2[M]\{q\} + [K]\{q\} = \{F_e\} + \{F_d\} \tag{33}$$

Again not all the displacements in q are unknown, and therefore q will be divided into unknown displacements q_1 and specified displacements q_2.

Using Eq. (32) in (33) and partitioning according to the q_1 and q_2 displacements, it follows that

$$-\omega^2\begin{bmatrix} M_1 & M_2 \\ M_3 & M_4 \end{bmatrix}\begin{Bmatrix} q_1 \\ q_2 \end{Bmatrix} + \begin{bmatrix} K_1 & K_2 \\ K_3 & K_4 \end{bmatrix}\begin{Bmatrix} q_1 \\ q_2 \end{Bmatrix} = \begin{Bmatrix} F_{1e} \\ F_{2e} \end{Bmatrix} + \begin{bmatrix} D' + iD'' & 0 \\ 0 & D' + iD'' \end{bmatrix}\begin{Bmatrix} q_1 \\ q_2 \end{Bmatrix} \tag{34}$$

The unknown displacements q_1 are divided into real and imaginary parts:

$$q_1 = q_{1R} + iq_{1I} \tag{35}$$

Using the above expression in Eq. (34), we obtain the following relation:

$$\{[N] - i[D'']\}\{q_{1R} + iq_{1I}\} = \{R\} \tag{36}$$

where matrices R and N are defined as:

$$\begin{aligned} \{R =\} &\{F_{1e}\} + \{\omega^2[M_2] - [K_2]\}\{q_2\} \\ [N] &= -\omega^2[M_1] + [K_1] - [D'] \end{aligned} \tag{37}$$

It may be noted that the matrices D' and D'' in Eqs. (36) and (37) represent only portion of the original damping matrix in Eq. (34). Equation (36) can be divided into real and imaginary parts and solved for the two unknown matrices q_{1R} and q_{1I}. The solutions are

$$\{q_{1R}\} = \{[N] + [D''][N]^{-1}[D'']\}^{-1}\{R\} \tag{38}$$

$$\{q_{1I}\} = [N]^{-1}[D'']\{[N] + [D''][N]^{-1}[D'']\}^{-1}\{R\} \tag{39}$$

Once the displacement matrices q_{1R} and q_{1I} are determined from Eqs. (38) and (39), the solution for forced vibration problem is completed since the response at each point is known. It may be observed that Eqs. (38) and (39) automatically reduce to the response of an undamped panel when D' and D'' matrices are specified as zero. The method of solution described here has been programed on a digital computer and examples of its application will be given later in the next section.

Table 1 Physical properties for free vibration example

Panel properties	Stringer properties
h = 0.04 in.	E = 10.5 × 10[6] lb/in.[2]
ν = 0.3	G = 4.03 × 10[6] lb/in.[2]
E = 10.5 × 10[6] lb/in.[2]	J = 2.263 × 10[−4] in.[4]
ρ = 0.004 lb/in.[2]	C_{ws} = 0.01649 in.[6]
	I = 0.254 in.[4]
	m = 0.02302 lb/in.

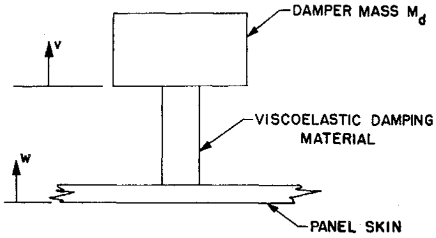

Fig. 4 Viscoelastic damper attached to the panel surface.

Numerical Examples

Free Vibration

As an example of the free vibration analysis, a model was chosen consisting of a rectangular panel stiffened by two parallel stiffeners that divide the panel into three bays as shown in Fig. 5. The panel is simply supported on its four edges. This example has been chosen because an exact solution is possible and has been obtained elsewhere by the transfer matrix method.[3] Having the exact solution permits us to illustrate the accuracy of the finite-element approach.

The physical properties of the structural model, shown in Fig. 5, are given in Table 1.

The results obtained by the finite-element analysis depend on the number of finite elements which are used in modeling the structure. A more accurate answer should be expected as the number of elements is increased, since this increases the degrees of freedom in approximating the continuous structure. In the present computer program there is an upper limit on the number of elements which is dictated by the core storage capacity of the computer. This limit is represented by the size of the stiffness and the mass matrices in Eq. (25), and in

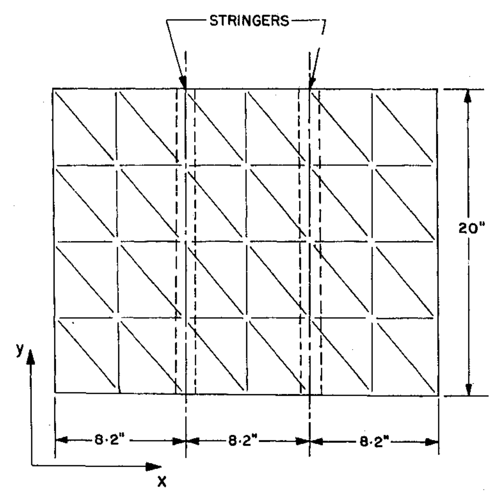

Fig. 5 Panel-stringer model used in the numerical examples.

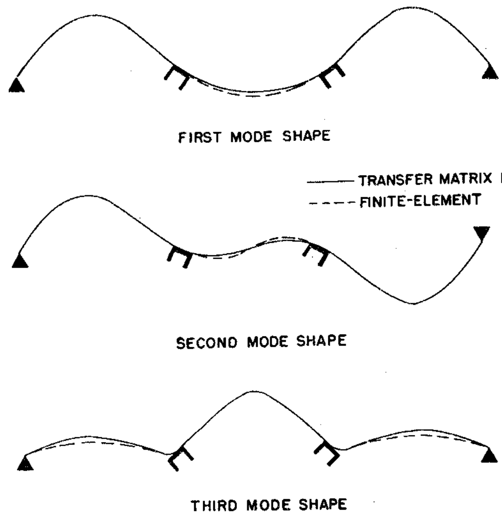

Fig. 6 Comparison of mode shapes calculated by transfer matrix and finite-element methods.

the present program this size is 145 × 145. Further increases in this size would require the use of external drum or disk storage facility which would appreciably increase the computing time; however such a modification can easily be carried out in the present computer programs if it is needed. For this example a grid size was chosen consisting of five nodes in the x and seven in the y direction as shown in Fig. 5. The nodes were equally spaced in both directions. The calculations were performed using 200 iterations for each of the natural frequencies; this was found to yield very good convergence. The calculated natural frequencies for this example are 89.1, 91.5, and 118.0 cps. The corresponding values obtained by the transfer matrix method[3] are 85.5, 88.5, and 116.0. It can be seen that the respective errors for the three frequencies calculated by the finite-element method are 4.2, 3.4, and 1.25%. The mode shapes corresponding to these three frequencies are shown in Fig. 6, where the results from the finite-element method are compared with those from the transfer matrix analysis. In these plots the solid curves correspond to the transfer matrix method results and the dashed curves are from the finite-element analysis. In the places when only a solid curve is shown, the two methods agree closely and cannot be distinguished on the scale used in Fig. 6. The agreement between the two methods is seen to be good.

The free vibration model was also used to investigate the effect of omitting the warping effect from the structural representation of the stiffeners. In order to do this, the calculations were repeated using zero value for the warping constant C_{ws}. The three lowest natural frequencies for this case were found to be 74.5, 82.1, and 107.2 cps. Comparing these values with the previous calculations, where warping effect was included, it can be seen that this effect does indeed play an important part in the free vibration characteristics.

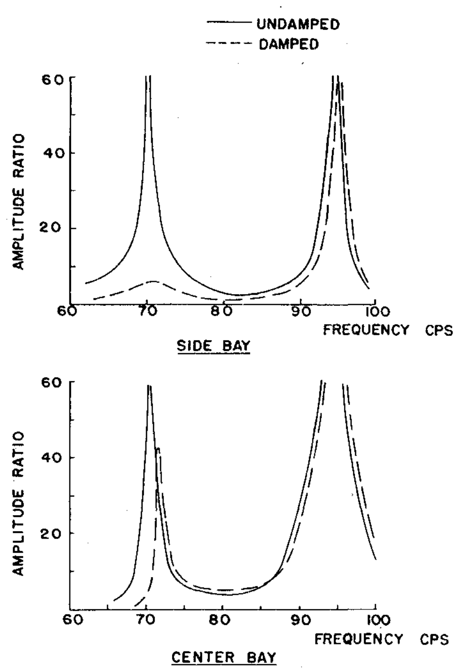

Fig. 7 Undamped and damped displacement response of side and center bays calculated by the finite-element method.

Forced Vibration

The forced vibration analysis was applied to an example to determine its frequency response under undamped and damped conditions. The structural model chosen for this study consists of a rectangular panel stiffened by two parallel stiffeners, and it has the over-all dimensions the same as those of the model shown in Fig. 5 and used previously in the free vibration analysis. The other physical properties of the panel are given in Table 2.

The configuration of this model was chosen so as to correspond to the configuration which was used in the experimental portion of this investigation, and the objective is to compare the theoretical and the experimental results. The three lowest natural frequencies were calculated by using the free vibration analysis and they were found to be 70.0, 72.5, and 94 cps. The forced vibration analysis was then used to evaluate the frequency response of this model for undamped and damped conditions. The damping was provided by a discrete damper which was tuned to the first natural frequency and attached to the central point of one of the side bays. The spring constant, viscous coefficient, and the mass of the damper had the following numerical values: 11.83 lb/in., 0.0052 lb/in./sec., and 0.0232 lb, respectively. The size of the finite-element grid used in the calculations was $X = 5$ and $Y = 7$. The frequency calculations were performed at approximately 1 cps intervals. The sinusoidal forcing was applied by specifying a uniform transverse displacement on the periphery of the model, and the edge conditions were assumed to be simply-supported. The results of these calculations are shown in Fig. 7 where the displacement ratio, defined as the displacement divided by edge input displacement, is given as a function of frequency. The results show the response for the central points on the side and the center bays of the model. The results in Fig. 7 compare the response obtained for the undamped and damped conditions. The undamped conditions result in a response with two sharp peaks which can be seen to correspond to the first and third natural frequencies. The second natural frequency did not affect the response, because it corresponds to an unsymmetric mode shape that did not respond to the input which was symmetric with respect to the center panel. The unsymmetry produced by placing a damper on a side panel did not alter this behavior noticeably. The top diagram in Fig. 7 shows the effect of the damper on the side bay to which the damper is attached. It can be seen that the damper is very effective in reducing the displacement in the neighborhood of the first natural frequency; whereas much less effect is seen around the third natural frequency

Table 2 Physical properties for forced vibration example

Panel properties	Stringer properties
$h = 0.032$ in.	$E = 10.5 \times 10^6$ lb/in.^{2}
$\nu = 0.3$	$G = 4.03 \times 10^6$ lb/in.^{2}
$E = 10.5 \times 10^6$ lb/in.^{2}	$J = 2.03 \times 10^{-4}$ in.^{4}
$\rho = 0.0032$ lb/in.^{2}	$C_{ws} = 0.0067$ in.^{6}
	$I = 0.144$ in.^{4}
	$m = 0.016$ lb/in.

The corresponding results for the central bay are shown in the bottom diagram of Fig. 7. It can be seen that the effect of the damper, still attached to the side bay, is much less for this adjacent bay even in the neighborhood of the first frequency.

The experimental program was designed to duplicate the aforementioned theoretical investigation. The test model was constructed of aluminum, and its dimensions and properties were chosen as to correspond as closely as possible to the model used in the numerical calculations. The test model was mounted on its periphery on thick aluminum plate which served as a rigid base. The forcing was applied to this plate by a 1200-lb force sinusoidal, electromagnetic shaker. The discrete damper was constructed from a silicon rubber material RTV 631, and the properties of the damper were chosen as to correspond to the measured first natural frequency of the model. It was found that in the frequency range of interest it was possible to characterize the damping material by a single spring-dashpot model. The response of the model was measured by a piezoelectric accelerometer which was attached by double-back tape to the model. The mass of the accelerometer used was only 0.5 g, and it was found to have a negligible effect on the panel response. The experimental results are shown in Fig. 8. These results correspond directly to the theoretical results given in Fig. 7. By comparing these two figures one basic difference is immediately obvious. The undamped experimental response exhibits three peaks which correspond to the first three natural frequencies. It was found that, unlike in the theoretical analysis, the experimental model did respond in the second natural frequency. This is in spite of the effect that both the model and the forcing input were symmetric. The explanation for this behavior must lay in the presence of sufficient amount of eccentricities, both in the model configuration and the forcing displacements, to produce the necessary unsymmetry. Of course another basic difference between Figs. 7 and 8 is the fact that the theoretical results predict displacements going to infinity at the natural frequencies when no damping is present. The experimental results illustrate the effect of the tuned damper, and again we see that the damping effect is strong on the side bay in the vicinity of the first natural frequency. The third natural frequency peak on the same bay is not affected. The response of the center panel is not affected even at the first frequency. These are similar results to those obtained from the theoretical analysis.

Conclusions

The method of the finite elements has been developed and shown to be effective in predicting the free and forced vibration of orthogonally stiffened flat panels. The numerical examples illustrate the importance of including warping effects in the open-section stiffeners. In fact, the warping effects can be shown to provide most of the torsional stiffness for such sections. The advantage of the finite-element approach is, of course, in the area of analysis of complicated structural models and the method can handle much more general configurations than considered in the examples presented here. The theoretical and experimental analyses of the forced vibration illustrate the effect of discrete, tuned dampers on the amplitude of the response. The dampers are very effective in the frequency range in the vicinity of the tuned frequency and on the particular bay of the panel to which the damper is attached. This implies that the influence of the damper is very localized.

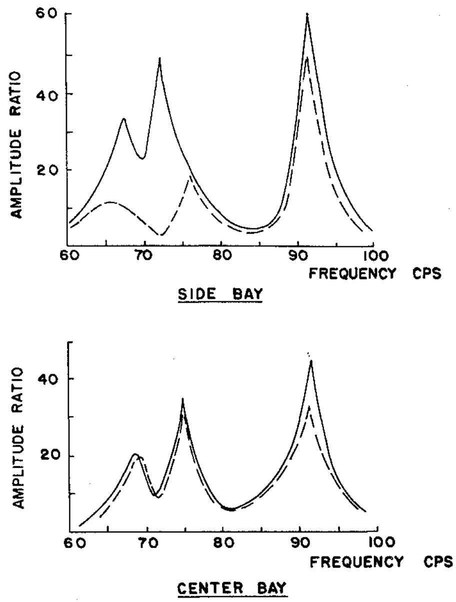

Fig. 8 Experimental results for the undamped and damped response of side and center bays.

References

[1] Lin, Y. K., "Free Vibration of Continuous Skin-Stringer Panels," *Journal of Applied Mechanics*, Dec. 1960, Vol. 27, No. 4, p. 669.

[2] Lin, Y. K. et al, "Free Vibration of Continuous Skin-Stringer Panels with Nonuniform Stringer Spacing and Panel Thickness," AFML-TR-64-347, Feb. 1965, Air Force Systems Command, Wright-Patterson Air Force Base, Ohio.

[3] Lin, Y. K. and McDaniel, T. J., "Response of Multi-Spanned Beam and Panel Systems Under Noise Excitation," AFML-TR-64-348, Sept. 1967, Air Force Systems Command, Wright-Patterson Air Force Base, Ohio.

[4] McDaniel, T. J., "Vibrations of a Stringer-Panel Structure with Mass Loading," AFML-TR-68-294, March 1969, Air Force Systems Command, Wright-Patterson Air Force Base, Ohio.

[5] Jones, D. I. G., "Effect of Isolated Tuned Dampers on Response of Multispan Structures," *Journal of Aircraft*, Vol. 4, No. 4, July-Aug., 1967, pp. 343–346.

[6] Jacobs, L. D. and Langerquist, D. R., "A Finite Element Analysis of Complex Panel Response to Random Loads," AFFDL-TR-68-44, Oct. 1968, Air Force Systems Command, Wright-Patterson Air Force Base, Ohio.

[7] Lindberg, G. M. and Olson, M. D., "Vibration Modes and Random Response of Multi-Bay System Using Finite Elements," Aeronautical Rept. LR-492, Dec. 1967, National Research Council of Canada, Ottawa, Canada.

[8] Lin, Y. K., *Probabilistic Theory of Structural Dynamics*. McGraw-Hill, New York, 1967.

[9] Lin, Y. K. and Donaldson, B. K., "A Brief Summary of Transfer Matrix Techniques with Special References to the Analysis of Aircraft Panels," *Journal of Sound and Vibration*, Vol. 10, No. 1, 1969, pp. 103–143.

[10] Zienkiewicz, O. C., "The Finite Element Method in Structural and Continuum Mechanics," McGraw-Hill, London, England, 1967.

[11] Severen, R. T. and Taylor, P. R., "Plate Vibration Problems Using the Finite Element Method with Assumed Distributions and Triangular Elements," *Proceedings on Numerical Methods for Vibration Problems*, University of Southampton, Vol. 3, 1966.